Proceedings of the
44th IEEE Conference on Decision and Control, and
the European Control Conference 2005
Seville, Spain, December 12-15, 2005

A Novel Hybrid Angle Tracking Observer for Resolver to Digital Conversion

Reza Hoseinnezhad, Peter Harding

Abstract— **Resolvers are absolute angle transducers that are usually used for position and speed measurement in permanent magnet motors. An observer that uses the sinusoidal signals of the resolver for this measurement is called an Angle Tracking Observer (ATO). Current designs for such observers are not stable in high acceleration and high-speed applications. This paper introduces a novel hybrid scheme for ATO design, in which a closed-loop LTI observer is combined with a quadrature encoder. Finite gain stability of the proposed design is proven based on the circle theorem in input-output stability theory. Simulation results show that the proposed ATO design is stable in two cases where an LTI observer and an extended Kalman filter are unstable due to high speed and acceleration,. In addition, the tracking accuracy of our hybrid scheme is substantially higher than a single quadrature encoder.**

I. Introduction

DIGITAL signal processors have enabled sensorless control that reduces the total system operating cost by eliminating mechanical sensors while maintains the performance of the control system. However, there are still applications where sensorless control cannot achieve the required accuracy and reliability. This is especially true with respect to the angular position and speed. Examples include servo applications, like robotics and numerically controlled machine tools. Mechanical sensors used in such applications are usually incremental encoders and *resolver*s.

While incremental encoders are relative position sensors, resolvers are absolute angle transducers, providing two output signals that always allow the detection of the absolute angular position. In addition they suppress common mode noise. Therefore they are especially useful in a noisy environment. A resolver is basically a rotary transformer with one rotating reference winding (Supplied by U_{ref}) and two stator windings. The reference winding is fixed on the rotor, and therefore, it rotates jointly with the shaft passing the output windings. Two stator windings are placed in quadrature of one another and generate the sine and cosine voltages (U_{sin} and U_{cos}) respectively. The sine winding is phase advanced by 90° with respect to the cosine winding. Both windings will be further referred to as output windings.

In consequence of the excitement applied on the reference winding U_{ref} and along with the angular movement of the motor shaft Θ, the respective voltages are generated by resolver output windings U_{sin} and U_{cos}. The frequency of the generated voltages is identical to the reference voltage and their amplitudes vary according to the sine and cosine of the shaft angle Θ.

Formerly resolvers were used primarily in analog design in conjunction with a *Resolver Transmitter - Resolver Control Transformer* [1]. These systems were frequently employed in servomechanisms, e.g. in aircraft on board instrument systems. Modern systems, however, use the digital approach to extract rotor angle and speed from the resolver output signals. They are called *resolver to digital converters* (RTDs). Most of RTDs are either trigonometric or *angle tracking observers*.

In the trigonometric approach, the shaft angle is determined by an *Inverse Tangent* function of the quotient of the sampled resolver output voltages U_{sin} , U_{cos}. This approach can be implemented by different DSP chips, e.g. Texas Instrument's TMS320F240 [2]. Modern control algorithms for electric drives require knowledge of both the rotor angle and the rotor speed. The trigonometric method, however, only yields values of the unfiltered rotor angle without any speed information. Therefore, for a final application, a speed calculation with smoothing capability should be added. This drawback is eliminated if a special *angle-tracking observer* (ATO) is utilized.

A great advantage of the ATO method, compared to the

Manuscript received September 15, 2005.

Reza Hoseinnezhad is a postdoctoral research fellow at the Faculty of Engineering and Industrial Sciences, Swinburne University of Technology, John street, Hawthorn, Victoria 3122, Australia (phone: +61-3-9214-8755; fax: +61-3-9214-8264; e-mail: rhoseinnezhad@ swin.edu.au).

Peter Harding is a control engineer at Pacifica Group Technologies Pty Ltd., 264 East Boundary Road, East Bentleigh, Victoria 3165, Australia (e-mail: peter_harding@pgt.com.au).

0-7803-9568-9/05/$20.00 ©2005 IEEE

trigonometric method, is that it smoothly and accurately tracks both the rotor angle and the rotor speed [3]. So far, different ATO designs have been developed for different applications. Fig. 1 shows a common schematic diagram that applies to all ATO designs. The resolver output signals are compared to their corresponding estimations $\hat{U}_{sin}$, $\hat{U}_{cos}$. If $\theta - \hat{\theta}$ (the observer error) is small, then $\sin(\theta - \hat{\theta}) \approx \theta - \hat{\theta}$. By this simplifying assumption, the ATO closed-loop transfer function is given by:

$$\frac{\hat{\Theta}(s)}{\Theta(s)} = \frac{G(s)}{s + G(s)} . \quad (1)$$

The open-loop transfer function G(*s*) is designed in such a way that the above transfer function is stable. Thus the nonlinear closed-loop observer in Fig. 1 will be asymptotically stable around $\theta - \hat{\theta} = 0$. The Motorola design [4] uses a DSP56F80x for hardware interfacing of a resolver driver. In this ATO design, the following choice for G(*s*) in Fig. 1 is selected:

$$G(s) = K_1(K_2 + 1/s) \quad (2)$$

that is indeed a PI observer, cascaded with an integrator to remove the steady-state error from ramp responses.

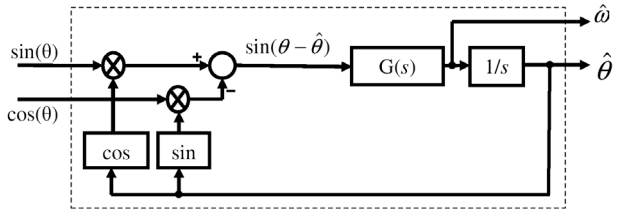

Fig. 1. A common schematic diagram of different designs for Angle Tracking Observers

In other trials, different transfer functions have been selected. For example Harnefors utilised an extended Kalman filter [5] and in Ellis and Krah's design a Luenberger observer was developed for angle tracking [6]. In both cases, the derived observers had the structure shown in Fig. 1, with the following form of open-loop transfer functions:

$$G(s)/s = \left(K_1 s^2 + K_2 s + K_3\right)/s^3 . \quad (3)$$

There is, however, a critical issue with the general diagram of ATO design shown in Fig. 1. Despite the open-loop observer is linear time invariant - LTI (we call it LTI-ATO design henceforward), the closed-loop design is nonlinear (because of the sine and cosine elements) and its stability is not guaranteed. Indeed, the tracking error of such an observer will be bounded only for a limited speed and acceleration. Our experiments show that in case of high rotor speed or high acceleration, the LTI-ATO outputs diverge toward infinity. In addition, both the trigonometric and the LTI-ATO methods of angle tracking are sensitive to noise and cannot compensate for the imperfections in resolver sinusoidal signals.

In this paper, we present a novel hybrid ATO design that is stable for a wide range of rotor speed and acceleration. In the next section our proposed observer is explained and its input-output stability is mathematically proven. Simulation results are presented in section III and section IV concludes this paper.

II. Proposed Angle Tracking Observer and Its Stability Analysis

In order to avoid divergence, the output of the LTI-ATO is fused with the output of a quadrature encoder that tracks the angle with a maximum error of ±45º. This quadrature encoder is implemented by two Schmitt triggers that trigger their states at the zero crossing points of the U_{sin} and U_{cos} respectively, and a counter that counts the number of zero crossing points from the Schmitt triggers' output signals. The output of such a quadrature encoder, disregarding the noise and the narrow hysteresis band of the Schmitt triggers, can be expressed as the following function of the rotor angle:

$$\theta_{quad} = \frac{\pi}{2} N_{quad} = \frac{\pi}{2}\left[\left(\theta + \frac{\pi}{4}\right) \Big/ \frac{\pi}{2}\right] \quad (4)$$

where [.] means "rounding to the nearest integer towards minus infinity".

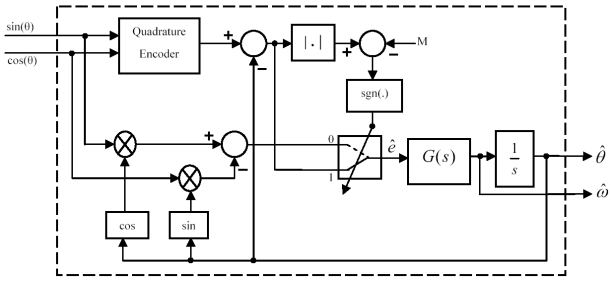

Fig. 2. The block diagram of our proposed Angle Tracking Observer: The input of the open-loop observer (i.e. G(*s*)/*s*) is a switched error signal that is either the tracking error provided by the LTI-ATO or the quadrature encoder.

A. Our Proposed Angle Tracking Observer

Due to its zero crossing counting nature, the quadrature encoder tracks the rotor position robustly but inaccurately. The block diagram of our proposed method is shown in Fig. 2 where |.| means "absolute value", sgn(.) is zero for negative and one for positive or zero argument, and *M* is a switching threshold. The input to the open loop observer is an error signal $\hat{e}(t)$ given by the following equation:

$$\hat{e}(t)=\begin{cases}\sin(\theta(t)-\hat{\theta}(t)) & \text{if } \left|\theta_{\text{quad}}(t)-\hat{\theta}(t)\right|<M \\ \theta_{\text{quad}}(t)-\hat{\theta}(t) & \text{otherwise}\end{cases}. \quad (5)$$

The outputs of this closed-loop observer design are the rotor position and speed. The error signal given to the feed-forward path is initially same as it is in a LTI-ATO design. When the observer approaches an unstable condition, this error signal is switched to another signal that is constructed based on the difference between the angle estimate and the quadrature encoder output. This difference is continually calculated by the ATO and the switching action takes place if its absolute value is greater than the threshold *M*.

Depending on the frequency response of the open-loop observer, *finite gain stability* of the angle-tracking observer can be guaranteed for some values of switching threshold *M*. This inturn ensures that our proposed angle tracking method will never diverge and lose its lock to the real rotor angle.

B. Stability Analysis

Before starting our analysis approach, some preliminary definitions and lemmas of the theory of input-output stability are presented as follows:

Definition 1: A system is *finite gain stable* if there is a constant positive gain γ such that:

$\|y_\tau\| \le \gamma \|u_\tau\|$; for all τ (6)

where $u(t)$ and $y(t)$ are the input and output signals of the system respectively, ||.|| is a norm function (e.g. 2-norm or ∞-norm) and u_τ denotes the truncated signal defined as equal to $u(t)$ in [0,τ] and zero in (τ, ∞) [7].

Finite gain stability of a system guarantees it output convergence with limited tracking error. This is the main feature of our proposed ATO that is proven in this section. There are different methods to investigate finite gain stability of a closed-loop system including the methods based on small-gain [8], passivity [9] and circle ([8]-[12]) theorems.

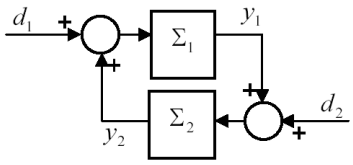

Fig. 3. Standard feedback configuration

Since the transfer function of the open loop observer always has at least one pole at the origin (for the sake of removing the steady state error), the necessary conditions for small-gain and passivity theorems are not satisfied in our case of study. Thus, we will study our system stability based on the circle theorem as explained in the following.

Input-output stability analysis methods are usually expressed and formulated for the standard feedback configuration, shown in Fig. 3.

Definition 2: A memoryless nonlinearity with input u and output $\varphi(u,t)$ belongs to SECTOR[-(*c*+*r*),-(*c*-*r*)] if it satisfies:

$| \varphi(u,t)+cu| \le |ru|$; for all t , u (7)

where $c \ge 0$, $r \ge 0$ ([7],[8]).

Schematically, in the case of $c>r$, if a memoryless nonlinearity belongs to SECTOR[-(*c*+*r*),-(*c*-*r*)] then its graph (its output plotted versus its input) will fall within the shaded area in Fig. 4.

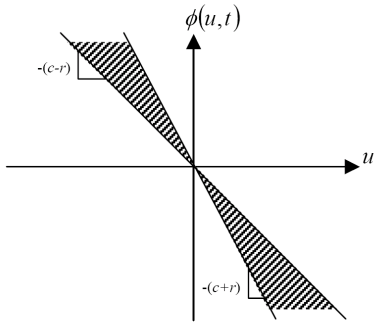

Fig. 4. A schematic diagram of SECTOR[-(*c*+*r*),-(*c*-*r*)] defined in Definition 2 for the case of $c>r$.

Circle Theorem: Consider a closed-loop system with the standard feedback configuration, shown in Fig.3. If Σ_2 is a SISO system having a real, rational transfer function $G_O(s)$ and Σ_1 is a memoryless nonlinearity belonging to SECTOR[-(*c*+*r*),-(*c*-*r*)] and one of the following conditions are met, then the close-loop system is finite gain stable:

C1: $r > c$ and $G_O(s)$ is stable and its Nyquist plot lies in the interior of the circular disc in the complex plane centred on the real axis and passing through the points on the real axis with real parts -1/(*c*+*r*) and -1/(*c*-*r*) (denoted by $D_{c,r}$).

OR

C2: $r = c$ and $G_O(s)$ is stable and its Nyquist plot is bounded away and to the right of the vertical line passing through the real axis at the value -1/(*c*+*r*).

OR

C3: $r < c$ and the Nyquist plot of $G_O(s)$ (with Nyquist path indented into the right-half plane) is outside of and bounded away from the disc $D_{c,r}$ and the number of times the plot encircles this disc in the counter-clockwise direction is equal to the number of poles of $G_O(s)$ with strictly positive real parts.

Proof: Refer to section 6.8 of Marquez's book [8] or each of the Sandberg's papers [10]-[12].

In Fig. 5, we have redrawn our proposed close-loop

angle-tracking observer in the form of the standard feedback configuration. The transfer function $G_O(s)$ stands for the open-loop observer, i.e. $G(s)/s$ in Fig. 2. Σ_1 is a memoryless nonlinearity whose input is the error signal $e(t) = \theta(t) - \hat{\theta}(t)$ and its output is $-\hat{e}(t)$, which is given, using (5), by the following nonlinear function of its input:

$$-\hat{e}(t) = \begin{cases} -\sin(e(t)) & \text{if } \left|e(t) + \theta_{\text{quad}}(t) - \theta(t)\right| < M \\ -\left(e(t) + \theta_{\text{quad}}(t) - \theta(t)\right) & \text{otherwise} \end{cases}. \quad (8)$$

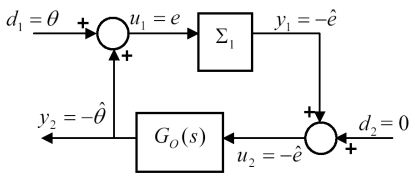

Fig. 5. The block diagram of our proposed ATO, redrawn in the form of a standard feedback configuration ($G_O(s)=G(s)/s$)

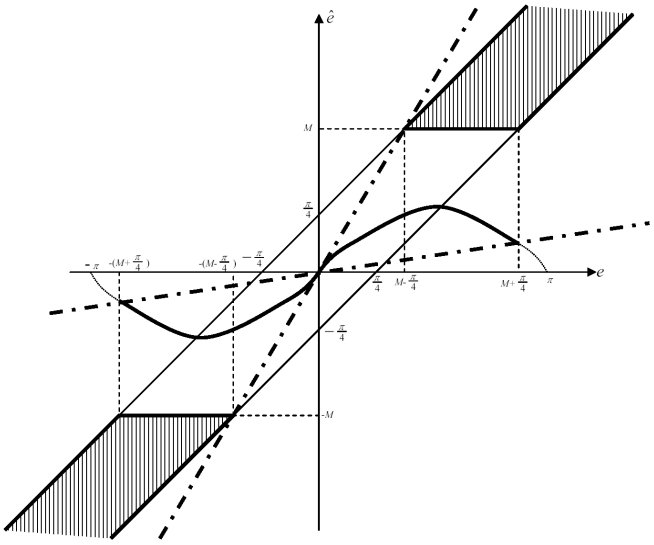

Fig. 6. Graph of the nonlinearity $-\Sigma_1$ (the solid black sinusoidal curve and the shaded area): Since $\hat{e}(t)$ has been plotted versus $e(t)$ and the output of Σ_1 is $-\hat{e}(t)$, the actual graph of Σ_1 can be easily derived by reflecting the above graph with respect to the horizontal axis. The two dotted lines indicate the conic sector to which the graph belongs.

Fig. 6 shows the graph of Σ_1 (its output signal plotted versus its input). The term $\theta_{\text{quad}}(t) - \theta(t)$ in (8) is the quadrature encoder error. Equation (4) shows that this error is never higher than $\pi/4$. Due to this term in (8), the graph of Σ_1 includes a shaded area. Fig. 6 shows that in our closed-loop observer, Σ_1 belongs to a conic sector in the form of SECTOR$[-(c+r),-(c-r)]$ as defined in Definition 2, with the following parameter values:

$$c + r = \frac{M}{M - \frac{\pi}{4}} \quad ; \quad c - r = \frac{\sin(M + \frac{\pi}{4})}{M + \frac{\pi}{4}}. \quad (9)$$

As expressed before, to remove the steady state errors, the open loop observer transfer function $G_O(s)$ always has at least one pole at the origin. Thus $G_O(s)$ is not stable and the conditions C1 and C2 do not apply. The condition C3, however, can be satisfied and should be investigated.

Based on the circle theorem, the sufficient condition for finite gain stability of the closed loop ATO design in Fig. 2 is that the Nyquist plot of $G_O(s)$ (with Nyquist path indented into the right-half plane) is outside of and bounded away from the circular disc in the complex plane centred on the real axis and passing through the points on the real axis with real parts $-(M-\pi/4)/M$ and $-(M+\pi/4)/\sin(M+\pi/4)$, denoted by D_M. Furthermore the number of times the plot encircles D_M in the counter-clockwise direction should be equal to the number of poles of $G_O(s)$ with strictly positive real parts.

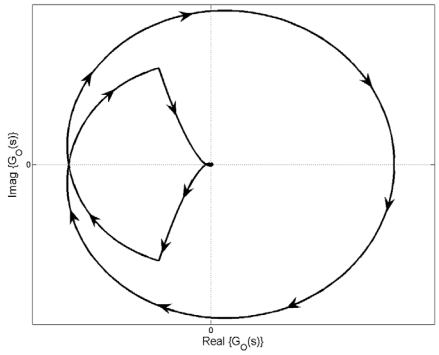

Fig. 7. Complete Nyquist plot of the $G_O(s)= G(s)/s$ given by (10), with the Nyquist path indented into the right-half plane

III. SIMULATION RESULTS

In our simulation studies, we compared the tracking performance of three techniques. The first method was an observer design based on extended Kalman filtering [5]. The other two methods included a LTI-ATO and our proposed ATO design design (Fig. 2). Both our ATO and the LTI-ATO used the following transfer function in their forward path:

$$G(s) = \frac{25s^2 + 211s + 915}{s^2} \quad (10)$$

Since $G_O(s)= G(s)/s$ has no poles with strict positive real parts, its Nyquist plot should not encircle the disc D_M. Fig. 7 shows the Nyquist plot of $G_O(s)$, with Nyquist path indented into the right-half plane. It is observed that a disc can be found encircled by the Nyquist plot once in clockwise and once in counter-clockwise direction. The Nyquist plot has been zoomed in, around origin in Fig. 8

with the disc $D_{\pi/2}$ also plotted. The figure shows that based on circle theorem, the closed-loop ATO is finite gain stable and its output convergence is guaranteed for $M = \pi/2$.

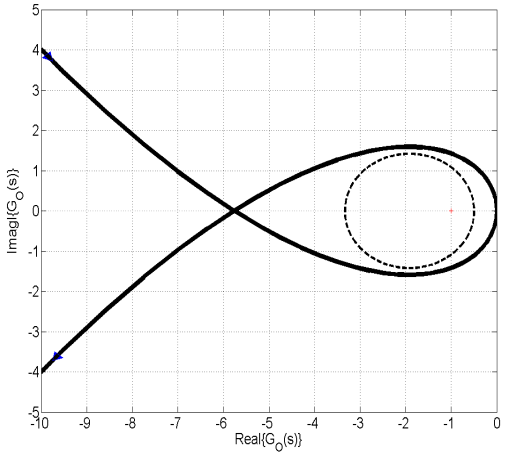

Fig. 8. The disc $D_{\pi/2}$ is inside the Nyquist plot.

Two cases of angle tracking were studied. In the first case, the angular position had a high constant acceleration of α=500 rad/sec^2. In the second case the angular position has a sinusoidal pattern, given by $\theta(t)=200\pi \sin(0.4\pi\, t)$ (rad). In this case the maximum angular acceleration of the rotor is 500 rad/sec^2. In order to see the effect of the noise on angle tracking performance, a white noise bounded within [-0.05,0.05] was added to the pure sine and cosine signals. This simulation was run for 80 seconds.

A. First Case: Constant High Acceleration

For the first case, the real angular position and its tracking using the LTI-ATO and the Kalamn filter are presented in Fig. 9. This figure shows that both techniques are unstable in case 1. However, our proposed observer, as proven in previous section, is stable and its tracking error converges to zero following a transient response. The position tracking error by our ATO design is shown in Fig. 10.

B. Second Case: Sinusoidal

Fig. 11 shows the real angular position and speed and their tracking using the LTI-ATO and Kalamn filter, for the second case. Again, this figure shows the instability of both the LTI-ATO and Kalman filter. The position tracking error using our ATO design is plotted in Fig. 12. While the position tracking error does not asymptotically approach to zero, it is bounded between ±2º, which is 18,000 times smaller than the amplitude of the sinusoidal waveform of the angular position that is under tracking.

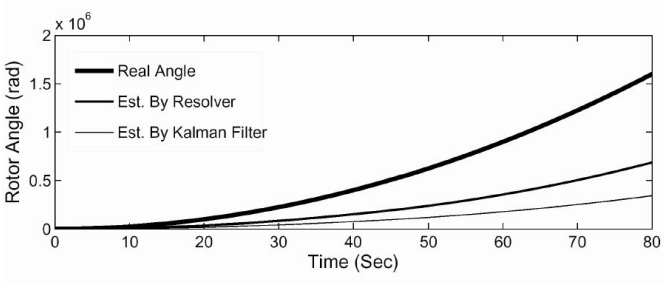

Fig. 9. The real and estimated angle, by the LTI-ATO (resolver) and Kalman filtering methods, in case 1

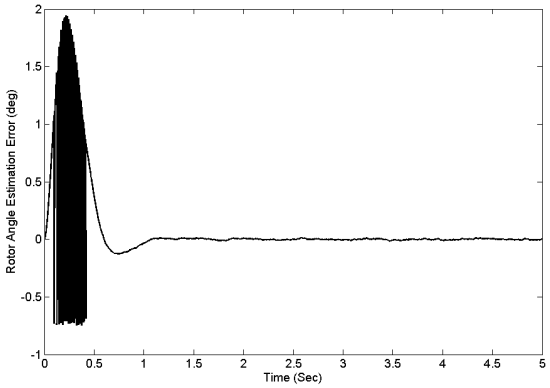

Fig. 10. Position tracking error with our proposed ATO in case 1: For clarity reason, the plot is shown in [0,5] seconds.

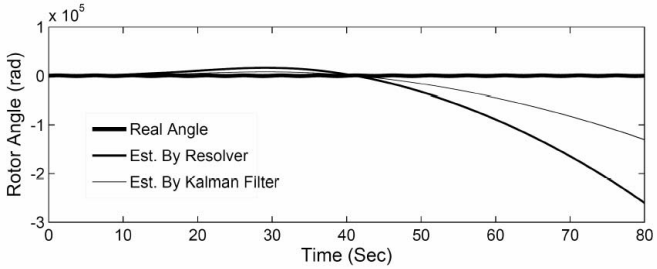

Fig. 11. Real and estimated angle, by the LTI-ATO (resolver) and Kalman filtering methods, in case 2

C. Hybrid Scheme Versus A Single Quadrature Encoder

As an angle tracking observer, a quadrature encoder has bounded-input bounded-output (BIBO) stability because its tracking error never exceeds $\pi/4$. However many angle tracking and control applications, require a higher accuracy than a single quadrature encoder. Our hybrid angle-tracking observer combines the quadrature encoder with a stable LTI-ATO.

A stable LTI observer will be asymptotically stable as well. Thus, the tracking error of this observer will approach to zero in steady state conditions. In other words, we expect

that the tracking performance of our new hybrid ATO is better than a singlequadrature encoder. In addition, a quadrature encoder does not directly track the speed and since its position output is discontinuous, the speed is not computable by direct differentiation of the estimated position.

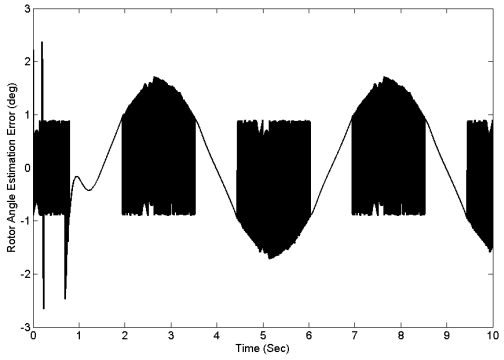

Fig. 12. Position tracking error with our proposed ATO in case 2: For clarity reason, the plot is shown in [0,10] seconds.

For a performance comparison, we calculated the mean square error (MSE) of the hybrid ATO and a single quadrature encoder. The MSE is defined as follows:

$$\text{MSE} = \sqrt{\frac{1}{T}\int_0^T \left(\theta(t) - \hat{\theta}(t)\right)^2 dt} \qquad (11)$$

where T is the simulation time. Table I presents the results of MSE calculation for each of the two simulation cases. It shows that as expected, our hybrid observer is significantly more accurate than a quadrature encoder.

TABLE I
COMPARISON OF MEAN SQUARE ERRORS BY A QUADRATURE ENCODER AND THE PROPOSED HYBRID SCHEME

	MSE In Case 1	MSE In Case 2
Quadrature Encoder	1.0992	1.3351
Hybrid ATO Scheme	0.0534	0.0955

IV. CONCLUSIONS

A new angle-tracking observer was introduced in this paper. In this hybrid design, the sine and cosine signal outputs of a resolver are processed in two different manners. On one side, they are combined with the output feedback of a LTI-ATO, providing the sinus of the tracking error. On the other side, their zero crossing points are counted by two Schmitt trigger units in a quadrature encoder that tracks the angular position with a maximum error of $\pi/4$. Depending on its magnitude, the tracking error is switched between the sine error of the LTI-ATO and the tracking error of quadrature encoder.

Finite gain stability of this hybrid design was proven based on circle theorem. Simulation studies comprised two cases where an LTI-ATO and an extended Kalman filter were unstable due to high acceleration and speed, and our proposed observer was stable with finite tracking errors. A comparative simulation study also showed that the tracking MSE of our closed-loop hybrid design is significantly lower than an open-loop single quadrature encoder.

This research project will continue with more analysis of robust stability of this hybrid observer and derivation of stability conditions in terms of the noise power in sine and cosine signals, and manufacturing variation. The stability and robustness of the observer and its tracking performance will also be examined through experimentation.

ACKNOWLEDGMENT

This research work was supported by Research Centre for Advanced By-Wire Technologies (RABiT) and Pacifica Group Technologies (PGT).

REFERENCES

[1] P. Kohl and T. Holomek, "Hollow shaft resolvers - Modern position sensors, ATAS Elektromotory a.s. Nachod," project report, 2000

[2] M. Staebler, "TM320F240 DSP solution for obtaining resolver angular position and speed," *Texas Instrument Application Report* SPRA605, February 2000. Available: www.eetkorea.com/ ARTICLES/2001MAY/2001MAY18_AMD_D SP_AN2.PDF

[3] D. Morgan, "Tracking demodulation," *Embedded Systems Programming*, no. 1, January 2001, pp. 115-120.

[4] M. Mienkina, P. Pekarek and F. Dobes, "DSP56F80x resolver, driver and hardware interface," *Motorola Inc. Application Report* AN1942/D, 2002. Available: http://www.freescale.com/files /product /doc/AN1942_D.pdf

[5] L. Harnefors, "Speed estimation from resolver noisy signals," in *Proc. IEE Conf. Power Electronics and Variable Speed Drives*, Sept. 1996, pp. 279-282.

[6] G. Ellis and J. O. Krah, "Observer-based Resolver Conversion in Industrial Servo Systems," in *Proc. PCIM 2001 Conference*, Nuremberg, Germany, 2001.

[7] A. R. Teel, T. T. Georgiou, L. Praly and E. Sontag, "Input-output stability," in *The Control Handbook*, 1st ed., W. S. Levine, Ed. Florida: CRC Press (in cooperation with IEEE Press), 1996, pp. 895-908.

[8] H. J. Marquez, *Nonlinear Control Systems: Analysis and Design*, Wiley Publishers, Chapter 6, April 2003.

[9] H. K. Khalil, *Nonlinear Systems*, Prentice Hall, 3rd Edition, 2002, Chapter 6.

[10] I. W. Sandberg, "A frequency-domain condition for the stability of feedback systems containing a single time-varying nonlinear element," *Bell System Tech. J.*, Vol. 43, No. 4, July 1964, pp. 1601-1608.

[11] I. W. Sandberg, "Some results on the theory of physical systems governed by nonlinear functional equations," *Bell System Tech. J.*, Vol. 44, No. 5, May-June 1965, pp. 871-898.

[12] I. W. Sandberg, "On the L-boundedness of solutions of nonlinear functional equations," *Bell System Tech. J.*, Vol. 43, No. 4, July 1964, pp. 1581-1599.